Electronic Research Archive

https://www.aimspress.com/journal/era

ERA, 34(9): 6404–6431.
DOI: 10.3934/era.2026280
Received: 28 May 2026
Revised: 01 July 2026
Accepted: 13 July 2026
Published: 20 July 2026

Research article

Dynamical behavior of a host–commensal system with multiplicative Allee effect and nonselective harvesting

Jinbo Zhang and Qin Yue*

School of Finance and Mathematics, West Anhui University, Lu'an 237000, China

* **Correspondence:** Email: yueqin@wxc.edu.cn.

Abstract: This paper studies a host–commensal model with a multiplicative Allee effect on the host and nonselective harvesting on both species. Exploiting the upper-triangular structure, equilibrium and stability analyses reduce to one-dimensional problems. Three harvesting thresholds corresponding to a fold and two transcritical bifurcations yield a complete classification of at most six equilibria. Global dynamics is determined via asymptotically autonomous systems: The separatrix $y = y_1$ divides coexistence and extinction basins at low harvesting, and the system collapses to monostability beyond the fold. Numerical simulations verify the three qualitatively distinct dynamical regimes.

Keywords: host–commensal model; multiplicative Allee effect; nonselective harvesting; upper-triangular structure; global dynamics; bistability; fold bifurcation; transcritical bifurcation

1. Introduction

Interspecific interactions are a fundamental object of study in theoretical ecology and mathematical biology. In addition to classical relationships such as predation, competition, mutualism, and parasitism, commensalism is also a widespread type of asymmetric interaction in nature: One species obtains benefits from another species, while the latter is essentially unaffected. In recent years, commensalism models and their stability, bifurcations, and persistence have attracted sustained attention [1–6]. Relevant ecological examples include epiphytic plants attaching to host trunks, barnacles adhering to the body surfaces of whales, and certain animals obtaining shelter or feeding opportunities by associating with large hosts. For the ecological background and mathematical modeling of commensalism, see [7–12].

In classical population dynamics, logistic growth is the most commonly used assumption for intrinsic growth. However, at low population densities, difficulties in finding mates, reduced cooperative defense, impaired social behavior, and other factors may lead to a decline in the population growth rate, and may even result in negative growth when the density falls below a certain

critical value. This is the well-known Allee effect [13–15]. In a commensal system, the host population is the basis on which the commensal derives its benefits; therefore, whether the host itself is subject to the Allee effect directly influences the long-term fate of both populations. A number of works have studied the influence of the Allee effect on commensalism and other asymmetric interaction systems [16–20]. Among them, Georgescu et al. [21] used the theory of asymptotically autonomous systems to study a commensalism model with a multiplicative Allee effect and revealed a bistable structure induced by the threshold effect.

In population models, the Allee effect is typically modeled in two forms: additive and multiplicative. The multiplicative Allee effect typically multiplies the logistic term by a factor

$$\left(\frac{y}{A} - 1\right),$$

thereby introducing an explicit critical threshold A: When the population density is below A, the net growth rate is negative; only when the density exceeds this threshold can the population recover and grow [22–26]. Such a hard threshold structure naturally induces basin separation and bistability phenomena. For a commensal system, if the host is affected by a multiplicative Allee effect, low host density will not only cause the host itself to go extinct; it may also indirectly lead to the decline of the commensal that depends on the host for its benefit. Therefore, imposing the multiplicative Allee effect on the host rather than on the commensal is a problem of clear ecological significance.

On the other hand, harvesting is an important means by which humans intervene in ecosystems. Nonselective harvesting generally refers to the situation where the same harvesting effort acts on multiple populations in the system simultaneously, rather than targeting only a particular species. The actual harvesting mortality of different species may differ due to different catchability coefficients; hence, the ecological effects can still be heterogeneous. The impact of harvesting on population models has been extensively studied in the fields of fisheries, forestry, and wildlife management [27–29]. In the presence of the Allee effect, the impact of harvesting is particularly noteworthy, because harvesting continuously reduces population density, making the population more likely to fall below the Allee threshold, thereby triggering irreversible population collapse [30–33].

The work closest to the present paper is that of Quansah and Ibrahim [1] on a commensalism model with ratio-dependent functional response and nonselective harvesting. They established conditions for the positivity, boundedness, and local and global stability of equilibria, and discussed the influence of harvesting and partial closure on the long-term behavior of the system. However, their host equation adopts pure logistic growth, so the host subsystem itself does not contain an Allee threshold structure. Consequently, the system mainly exhibits a monotonic degradation process from coexistence to a boundary state or extinction, making it difficult to capture the bistability phenomenon caused by differences in initial host density. To the best of our knowledge, works that simultaneously incorporate the host-multiplicative Allee effect and nonselective harvesting into a commensalism model, and that systematically analyze their equilibria, global basins of attraction, and bifurcation structure, remain scarce. The present paper aims to contribute an analysis in this direction.

In this paper, we consider the following two-dimensional autonomous ordinary differential equation (ODE) system:

$$\begin{cases} \dfrac{dx}{dt} = rx\Big(1 - \dfrac{x}{K}\Big) + \dfrac{bxy}{ay + x} - mq_1Ex \equiv F(x, y), \\ \dfrac{dy}{dt} = sy\Big(1 - \dfrac{y}{L}\Big)\Big(\dfrac{y}{A} - 1\Big) - mq_2Ey \equiv G(y). \end{cases} \tag{1.1}$$

A central structural feature of Model (1.1) is that the host dynamics, governed by $G(y)$, does not depend on the commensal variable x. This means that the host dynamics can be analyzed independently as a one-dimensional autonomous equation, and the commensal equation, once the host trajectory is given, becomes an asymptotically autonomous equation (approaching an autonomous limit system as $t \to \infty$). Apart from the ratio-dependent term at the origin (which requires separate treatment), the Jacobian matrix of the system is always upper-triangular, so its eigenvalues are given directly by its two diagonal entries. This structure significantly simplifies the local stability analysis and allows us, with the aid of the theory of asymptotically autonomous systems [34, 35], to reduce the ω-limit set analysis of the two-dimensional system to the dynamics of a one-dimensional limit system. Similar ideas have been used in studies of triangular ecological models with harvesting or commensal benefit terms [36].

The main contributions of this paper can be summarized as follows. First, exploiting the triangular structure of the model, this paper provides a complete classification of the existence and local stability of all equilibria. It shows that the dynamics are jointly determined by three critical harvesting thresholds m_1^*, m_2^*, m_3^* and their relative ordering. Second, by means of the theory of asymptotically autonomous systems and the ω-limit set method, this paper proves that the multiplicative Allee effect generates a threshold separation in the host dimension (the y-direction), thereby inducing a bistable structure in the two-dimensional system: When the initial host density lies on different sides of the Allee threshold, the system converges to different long-term ecological states. Finally, this paper analyzes the fold bifurcation and transcritical bifurcations caused by variations in harvesting intensity, revealing how nonselective harvesting, by altering the host threshold structure and the commensal growth conditions, causes the system to transition from bistability to monostability.

The structure of this paper is organized as follows. Section 2 presents the biological meaning of each term in the model and defines the three critical harvesting thresholds. Section 3 discusses the classification of equilibrium existence. Section 4 analyzes the local stability of each equilibrium. Section 5 uses the asymptotic autonomous limit lemma and the ω-limit set method to establish a global dynamical classification and the separatrix of basins of attraction. Section 6 analyzes the bifurcation behavior at the three critical thresholds. Section 7 verifies the theoretical results through numerical examples. Section 8 summarizes the paper and discusses the ecological significance of the model and possible directions for generalization.

Table 1. Nomenclature of state variables and parameters in the host–commensal model.

Symbol	Type	Description	Units
$x(t)$	State variable	Commensal population density	Biomass (or individuals/area)
$y(t)$	State variable	Host population density	Biomass (or individuals/area)
r	Parameter	Intrinsic growth rate of the commensal	Time^{-1}
K	Parameter	Environmental carrying capacity of the commensal	(Same as x)
s	Parameter	Intrinsic growth rate of the host	Time^{-1}
L	Parameter	Environmental carrying capacity of the host	(Same as y)
A	Parameter	Allee threshold of the host ($0 < A < L$)	(Same as y)
b	Parameter	Maximum benefit rate from host to commensal	Time^{-1}
a	Parameter	Half-saturation constant of the ratio-dependent response	(Same as x)
E	Parameter	Base harvesting effort	Effort units
m	Parameter	Harvesting effort scaling factor ($m \geq 0$)	Dimensionless
q_1	Parameter	Catchability coefficient of the commensal	$\text{Effort}^{-1}\cdot\text{time}^{-1}$
q_2	Parameter	Catchability coefficient of the host	$\text{Effort}^{-1}\cdot\text{time}^{-1}$

2. Model description and critical thresholds

2.1. Biological meaning of each model term

Convention: $x(t)$ is the commensal density and $y(t)$ is the host density. The meaning of each term in Model (1.1) is as follows:

- $rx(1 - x/K)$: Logistic growth of the commensal (intrinsic growth rate r, carrying capacity K);
- $bxy/(ay + x)$: Benefit that the commensal derives from the host, modeled by a ratio-dependent functional response; see [1, 12] for details;
- mq_1Ex: Nonselective harvesting of the commensal (q_1 is the catchability coefficient, E is the base effort, and m is the harvesting effort scaling factor);
- $sy(1 - y/L)(y/A - 1)$: Growth of the host under a multiplicative Allee effect. In the model, the Allee effect is realized by multiplying the logistic growth term $(1 - y/L)$ by the factor $(y/A - 1)$. This is the hallmark of a multiplicative Allee effect; The factor $(y/A - 1)$ ensures that the growth rate is negative when $y < A$, and the factor $(1 - y/L)$ provides the upper carrying capacity;
- mq_2Ey: Nonselective harvesting of the host.

Remark 2.1. The ratio-dependent benefit term

$$\Phi(x, y) = \frac{bxy}{ay + x}$$

is formally undefined at the origin $(0, 0)$. In this paper, we adopt the following continuous extension on the non-negative quadrant:

$$\Phi(x, y) = \begin{cases} \dfrac{bxy}{ay + x}, & (x, y) \neq (0, 0), \\ 0, & (x, y) = (0, 0). \end{cases}$$

This extension is continuous on $\mathbb{R}^2_{\geq 0}$, so the system is well-defined on the non-negative quadrant. However, Φ is not C^1 at the origin; consequently, the local properties at the origin cannot be obtained directly from the Jacobian matrix in the usual sense. In this paper, when discussing the stability and bifurcations of $E_0 = (0, 0)$, we treat it separately by means of the limiting dynamics along the coordinate axes or directional growth rates.

Remark 2.2 (Ecological implication of the nondifferentiability at the origin)**.** The nondifferentiability of the ratio-dependent benefit term at $(0, 0)$ does not alter the ecological conclusions obtained in this paper. Indeed, the coordinate axes are invariant. On the host-free axis $y = 0$, the commensal equation reduces exactly to

$$\dot{x} = x\left(r - mq_1E - \frac{r}{K}x\right),$$

so the invasion threshold of the commensal in the absence of the host is precisely

$$m_2^* = \frac{r}{q_1E}.$$

On the other hand, when the host density is positive, and the commensal is rare, the per-capita growth rate of the commensal satisfies

$$\lim_{x\to 0^+} \frac{F(x, y)}{x} = r + \frac{b}{a} - mq_1E, \qquad y > 0,$$

which yields the coexistence invasion threshold

$$m_3^* = \frac{r + b/a}{q_1E}.$$

If one approaches the origin along paths $y = kx$ with $k > 0$, the directional per-capita growth rate is

$$r - mq_1E + \frac{bk}{ak + 1},$$

which lies between $r - mq_1E$ and $r + b/a - mq_1E$. Thus, the two thresholds m_2^* and m_3^* represent the extreme biologically meaningful invasion scenarios: invasion without a host and invasion in the presence of a positive host density. Consequently, the lack of C^1 smoothness at the origin requires careful mathematical treatment, but it does not invalidate the invasion thresholds, the basin separation, or the ecological interpretation of the model.

2.2. Three critical harvesting thresholds

$$m_1^* \equiv \frac{s(L-A)^2}{4ALq_2E}, \qquad \text{(Threshold for the existence of positive host equilibria)}$$

$$m_2^* \equiv \frac{r}{q_1E}, \qquad \text{(Threshold for the commensal to survive alone)}$$

$$m_3^* \equiv \frac{r+b/a}{q_1E}, \qquad \text{(Coexistence threshold)}$$

Clearly, $m_2^* < m_3^*$ (because $b/a > 0$). The relative magnitude of m_1^* with respect to the other two depends on the parameter values, giving rise to three possible orderings:

- Case A (Baseline): $m_1^* < m_2^* < m_3^*$;
- Case B: $m_2^* \le m_1^* \le m_3^*$;
- Case C: $m_3^* < m_1^*$.

Different orderings correspond to qualitatively different dynamics. This paper takes Case A ($m_1^* < m_2^* < m_3^*$) as the baseline case and develops the analysis accordingly. Note that

$$m_1^* < m_2^* \iff r > \frac{s(L-A)^2}{4AL} \cdot \frac{q_1}{q_2},$$

so this ordering holds when r is sufficiently large, or q_1/q_2 is sufficiently small. Cases B and C are stated alongside the baseline case in the corresponding theorems.

2.3. Structural features of the model

The host component $G(y)$ of the vector field does not depend on the commensal variable x, which directly implies the following:

i. The Jacobian matrix of the system is always upper-triangular, and its eigenvalues are precisely the diagonal entries J_{11} and J_{22}. This greatly simplifies the local stability analysis (Section 4);

ii. The host subsystem can be solved independently; its global dynamics is completely determined by the one-dimensional ODE $\dot{y} = G(y)$ (Proposition 5.4);

iii. The ω-limit set of the two-dimensional system can be reduced to that of a one-dimensional limit system via the asymptotic autonomous limit lemma (Lemma 5.5), thereby decomposing the two-dimensional global stability problem into a cascade of two one-dimensional problems.

In the broader context of dynamical systems, such a triangular structure falls within the class of upper-triangular cooperative systems (cooperative systems with triangular Jacobian) [37, 38]. Mathematically, this upper-triangular structure reflects the extreme asymmetry of commensalism: The host is completely unaffected by the commensal, and its ω-limit set can be characterized in detail by means of the spectral theory of monotone dynamical systems.

Remark 2.3 (Scope of the asymmetric commensalism assumption)**.** The assumption that the host is not affected by the commensal is an idealized form of commensalism. Its main purpose in the present work is to make the system triangular, thereby allowing a complete classification of equilibria, basins of attraction, and bifurcations. If a weak feedback from the commensal to the host is introduced, for example,

$$\dot{y} = sy\Big(1 - \frac{y}{L}\Big)\Big(\frac{y}{A} - 1\Big) - mq_2Ey + \eta R(x, y), \qquad 0 < |\eta| \ll 1,$$

then the exact triangular reduction is generally lost. Nevertheless, by the implicit function theorem and standard persistence results for hyperbolic equilibria, all hyperbolic equilibria and their local stability types are expected to persist for sufficiently small $|\eta|$, although their locations and basin boundaries will be perturbed. The fold and transcritical thresholds may also shift by $O(\eta)$. A rigorous global analysis of such weakly nontriangular commensal or mutualistic perturbations is an important extension beyond the scope of the present paper. We note that in the purely triangular case ($\eta = 0$), Proposition 5.2 rigorously excludes nonconstant periodic orbits. For small $\eta \neq 0$, the triangular structure is broken and the Bendixson-type argument no longer applies. In principle, a weak feedback could shift eigenvalues across the imaginary axis, potentially generating Hopf bifurcations and isolated limit cycles. A full investigation of such possibilities would require a separate dedicated analysis.

3. Complete classification of the existence of equilibria

3.1. Equilibria of the host subsystem

The host equation $\dot{y} = G(y)$ is independent of x and can be solved first.

Proposition 3.1 (Host equilibria)**.** *The solutions of $G(y) = 0$ on $\mathbb{R}_{\geq 0}$ are as follows:*

(i) $y = 0$ is always an equilibrium (host extinction state).

(ii) Nonzero equilibria are given by the quadratic equation

$$y^2 - (L + A)y + AL\Big(1 + \frac{mq_2E}{s}\Big) = 0, \tag{3.1}$$

whose discriminant is $\Delta_y(m) = (L - A)^2 - \dfrac{4ALmq_2E}{s}$.

- *If $0 \leq m < m_1^*$: $\Delta_y > 0$, and there are two distinct positive real roots*

$$y_{1,2}(m) = \frac{L + A}{2} \mp \frac{\sqrt{\Delta_y(m)}}{2},$$

  satisfying $0 < y_1 < \frac{L+A}{2} < y_2$.
- *If $m = m_1^*$: $\Delta_y = 0$, and there is a unique positive root $y_1 = y_2 = \frac{L+A}{2}$ (a double root).*
- *If $m > m_1^*$: $\Delta_y < 0$, and there are no positive real roots.*

Proof. Setting $G(y) = 0$ and factoring out the common factor y yields:

$$y\Big[s\Big(1 - \frac{y}{L}\Big)\Big(\frac{y}{A} - 1\Big) - mq_2E\Big] = 0.$$

If $y > 0$, the expression inside the square brackets must vanish. Expanding the product:

$$s\Big(1 - \frac{y}{L}\Big)\Big(\frac{y}{A} - 1\Big) = s\Big(\frac{y}{A} - 1 - \frac{y^2}{AL} + \frac{y}{L}\Big) = -\frac{s}{AL}y^2 + s\frac{L+A}{AL}y - s.$$

Setting this equal to mq_2E and multiplying both sides by $-AL/s$ yields (3.1).

The discriminant is computed as:

$$\Delta_y = (L-A)^2 - \frac{4ALmq_2E}{s},$$

and $\Delta_y \geq 0$ is equivalent to

$$m \leq \frac{s(L-A)^2}{4ALq_2E} \equiv m_1^*.$$

The product of the two roots is $y_1y_2 = AL(1 + mq_2E/s) > 0$, and their sum is $y_1 + y_2 = L + A > 0$; hence, whenever two real roots exist, they are simultaneously positive. Their ordering follows directly from the square-root expression.

Biological interpretation: y_1 is the harvesting-modified Allee threshold. When the host density is below y_1, the growth rate is negative, and the population converges to extinction; only when the density surpasses y_1 does the growth rate change from negative to positive, allowing the population to recover. y_2 is the environmental carrying capacity of the host. Increasing the harvesting effort m compresses the gap between y_1 and y_2; when m reaches m_1^*, the two merge and disappear at $(L + A)/2$. This is a classical **fold bifurcation**, meaning that the host population cannot sustain a positive equilibrium state under excessively strong harvesting pressure.

3.2. The commensal subsystem

For any fixed $y^* \geq 0$, the commensal equilibrium condition $F(x, y^*) = 0$ is equivalent to $x[r(1 - x/K) + by^*/(ay^* + x) - mq_1E] = 0$. The solution $x = 0$ always exists; positive solutions $x > 0$ satisfy a quadratic equation. To simplify notation, let $h \equiv mq_1E - r$ (the net harvesting mortality rate).

Proposition 3.2 (Positive commensal equilibrium)**.** *For a fixed $y^* \geq 0$, the positive equilibrium of the commensal satisfies the quadratic equation*

$$rx^2 + B(y^*)x + C(y^*) = 0, \tag{3.2}$$

where

$$B(y^*) \equiv ray^* + Kh = ray^* + K(mq_1E - r),$$

$$C(y^*) \equiv Ky^*(ah - b) = Ky^*a\Big(mq_1E - r - \frac{b}{a}\Big).$$

The discriminant is $\Delta_x(y^*) = B(y^*)^2 - 4rC(y^*)$.

(i) If $m < m_3^*$ (i.e., $mq_1E < r + b/a$), then $C(y^*) < 0$ holds for all $y^* > 0$. In this case, Eq (3.2) *has exactly one positive real root:*

$$x^*(y^*) = \frac{-B(y^*) + \sqrt{\Delta_x(y^*)}}{2r} > 0.$$

(ii) If $m = m_3^*$, then $C(y^*) = 0$. The equation degenerates to $x(rx + B) = 0$; besides $x = 0$, the only nonzero root is $x = -B/r$. However, because $h = b/a > 0$, we have $B(y^*) = ray^* + Kb/a > 0$ for all $y^* \geq 0$, so in fact no positive root exists.

(iii) If $m > m_3^*$, then $C(y^*) > 0$ for all $y^* > 0$. In this case, $h \equiv mq_1E - r > b/a > 0$, so $B(y^*) = ray^* + Kh > 0$ for all $y^* \geq 0$. By Vieta's formulas, the sum of the two roots is $-B/r < 0$, and their product is $C/r > 0$; hence, both roots are negative—no positive root exists.

Proof. We start from the expression inside the square brackets of $F(x, y^*) = 0$. Let $h = mq_1E - r$, so that $mq_1E = r + h$. Substituting yields

$$r\Big(1 - \frac{x}{K}\Big) + \frac{by^*}{ay^* + x} - r - h = 0 \implies -\frac{r}{K}x + \frac{by^*}{ay^* + x} - h = 0.$$

Multiplying both sides by $K(ay^* + x)$ and rearranging gives:

$$rx^2 + (ray^* + Kh)x + Ky^*(ah - b) = 0.$$

Substituting $h = mq_1E - r$ back yields (3.2).

(i) $m < m_3^* \iff mq_1E < r + b/a \iff a(mq_1E - r) - b < 0$; hence, $C(y^*) < 0$. By Vieta's formulas, $x_1x_2 = C/r < 0$, so the two roots have opposite signs; thus, there is exactly one positive root. Moreover, because $-4rC > 0$, $\Delta_x = B^2 - 4rC > B^2 \geq 0$, so the discriminant is always positive. The positive root is given explicitly by the formula above.

(ii) and (iii) follow by direct substitution.

3.3. Unified naming and existence conditions for the six equilibria

All possible equilibria of System (1.1) are denoted as follows.

Table 2. Naming and coordinates of the equilibria.

Symbol	Name	Coordinates
E_0	Total extinction	$(0, 0)$
E_1	Commensal-only survival	$(x_{\text{solo}}, 0)$
E_2	Allee threshold without commensal	$(0, y_1)$
E_3	Host-only survival	$(0, y_2)$
E_4	Coexistence at lower host equilibrium	$(x^*(y_1), y_1)$
E_5	Coexistence at upper host equilibrium	$(x^*(y_2), y_2)$

Here,

$$x_{\text{solo}} = K\left(1 - \frac{mq_1E}{r}\right),$$

and, when it exists,

$$x^*(y_i) = \frac{-B(y_i) + \sqrt{B(y_i)^2 - 4rC(y_i)}}{2r}, \qquad i = 1, 2,$$

with B and C defined in Proposition 3.2.

Theorem 3.3 (Existence of equilibria)**.** *The existence conditions for all equilibria of System* (1.1) *are summarized in Table 3.*

Proof. The origin E_0 exists trivially. For E_1, setting $y = 0$ gives the logistic equation with harvesting,

$$\dot{x} = x\left(r - mq_1E - \frac{r}{K}x\right),$$

so the positive commensal-only equilibrium exists if and only if $r - mq_1E > 0$, namely $m < m_2^*$.

For host equilibria, Proposition 3.1 shows that two positive host equilibria y_1, y_2 exist precisely when $m \le m_1^*$. These give the boundary equilibria E_2 and E_3. Finally, for each positive host equilibrium y_i, Proposition 3.2 shows that a unique positive commensal coordinate $x^*(y_i)$ exists precisely when $m < m_3^*$. This yields E_4 and E_5. No other equilibria are possible because every equilibrium must first satisfy $G(y) = 0$, and the possible non-negative roots of G have already been exhausted.

Table 3. Summary of existence conditions for equilibria.

Equilibrium	**Coordinates**	**Existence condition**
E_0	$(0, 0)$	Always exists
E_1	$(x_{\text{solo}}, 0)$	$m < m_2^*$
E_2	$(0, y_1)$	$m \le m_1^*$
E_3	$(0, y_2)$	$m \le m_1^*$
E_4	$(x^*(y_1), y_1)$	$m \le m_1^*$ and $m < m_3^*$
E_5	$(x^*(y_2), y_2)$	$m \le m_1^*$ and $m < m_3^*$

Table 4. Side-by-side comparison of the three parameter-ordering cases.

Case	Threshold ordering	Equilibrium-count sequence	Main ecological feature	Observable bifurcations
A	$m_1^* < m_2^* < m_3^*$	$6 \to 4 \to 2 \to 1$	Baseline case. The host fold occurs before the commensal-only transcritical threshold. After the fold, all positive host states disappear.	Fold at m_1^*; transcritical I at m_2^*; transcritical II lies after host collapse and is not observable in the positive-host phase portrait.
B	$m_2^* \le m_1^* \le m_3^*$	$6 \to 5 \to 3 \to 1$	An obligate-commensalism interval may occur: The commensal cannot survive alone but can still persist with a positive host.	Transcritical I at m_2^*; fold at m_1^*; transcritical II may be hidden if it occurs after the fold.
C	$m_3^* < m_1^*$	$6 \to 5 \to 3 \to 2 \to 1$	Coexistence equilibria disappear before the host fold; a host-only–extinction bistable phase may remain before complete collapse.	Transcritical I at m_2^*; transcritical II at m_3^*; fold at m_1^*.

The three cases in Table 4 show that the same three thresholds may be crossed in different orders. This ordering determines whether the system first loses positive host equilibria, loses commensal-only survival, or loses coexistence through the commensal invasion threshold.

4. Local stability analysis

4.1. Upper-triangular structure of the Jacobian matrix

Away from the origin, where the ratio-dependent term is differentiable, the Jacobian matrix of System (1.1) is

$$J(x,y)=\begin{pmatrix} J_{11} & J_{12} \\ 0 & J_{22} \end{pmatrix},$$

where

$$\begin{aligned} J_{11} &= r\left(1-\frac{2x}{K}\right)+\frac{bay^2}{(ay+x)^2}-mq_1E, \\ J_{12} &= \frac{bx^2}{(ay+x)^2}, \\ J_{22} &= G'(y). \end{aligned}$$

Thus the eigenvalues are the two diagonal entries J_{11} and J_{22}. This upper-triangular structure is the key reason why local stability can be classified explicitly.

Lemma 4.1 (Host-direction eigenvalue)**.** *Let $y^*>0$ satisfy $G(y^*)=0$. Then,*

$$J_{22}(y^*)=G'(y^*)=\frac{sy^*}{AL}(L+A-2y^*).$$

Consequently, when $0<m<m_1^*$,

$$G'(y_1)>0, \qquad G'(y_2)<0.$$

Proof. Differentiating $G(y)$ and using the equilibrium relation

$$s\left(1-\frac{y^*}{L}\right)\left(\frac{y^*}{A}-1\right)=mq_2E$$

gives the stated expression. Because

$$y_1=\frac{L+A-\sqrt{\Delta_y}}{2}, \qquad y_2=\frac{L+A+\sqrt{\Delta_y}}{2},$$

the signs follow immediately.

Lemma 4.2 (Commensal-direction eigenvalue)**.** *Let (x^*,y^*) be an equilibrium of System* (1.1).

(i) If $x^*>0$, then

$$J_{11}(x^*,y^*)=-x^*\left[\frac{r}{K}+\frac{by^*}{(ay^*+x^*)^2}\right]<0.$$

(ii) If $x^* = 0$, and $y^* > 0$, then

$$J_{11}(0, y^*) = r + \frac{b}{a} - mq_1E = q_1E(m_3^* - m).$$

Proof. For $x^* > 0$, the equilibrium equation $F(x^*, y^*) = 0$ gives

$$mq_1E = r\left(1 - \frac{x^*}{K}\right) + \frac{by^*}{ay^* + x^*}.$$

Substitution into J_{11} yields the first formula. The second follows by directly setting $x^* = 0$ and $y^* > 0$ in J_{11}.

Proposition 4.3 (Universal stability criterion)**.** *Whenever the corresponding equilibria exist, their local stability is as follows:*

(i) E_0: Along the invariant axes, the directional growth rates are

$$\lambda_x^{\text{axis}} = q_1E(m_2^* - m), \qquad \lambda_y^{\text{axis}} = -(s + mq_2E) < 0.$$

Hence E_0 is a saddle for $m < m_2^*$ and a stable node for $m > m_2^*$.

(ii) E_1: Whenever it exists, it is a stable node.

(iii) E_2: Because $G'(y_1) > 0$, it is an unstable node for $m < m_3^*$ and a saddle for $m > m_3^*$.

(iv) E_3: Because $G'(y_2) < 0$, it is a saddle for $m < m_3^*$ and a stable node for $m > m_3^*$.

(v) E_4: Whenever it exists, it is a saddle.

(vi) E_5: Whenever it exists, it is a stable node.

Proof. The assertions follow directly from Lemmas 4.1 and 4.2, together with the axis-based directional growth rates at the nondifferentiable origin.

Table 5. Local stability of equilibria in the baseline case $m_1^* < m_2^* < m_3^*$ and $0 < m < m_1^*$.

Equilibrium	Eigenvalue signs	Stability type	Ecological meaning
E_0	$(+, -)$	Saddle	Extinction is unstable to commensal invasion
E_1	$(-, -)$	Stable node	Commensal-only attractor
E_2	$(+, +)$	Source	Host Allee threshold
E_3	$(+, -)$	Saddle	Host-only state invaded by commensal
E_4	$(-, +)$	Saddle	Separatrix point
E_5	$(-, -)$	Stable node	Stable coexistence

For Cases B and C, no new local stability mechanism appears. The stability type of each equilibrium is still determined by Proposition 4.3; only the order in which the thresholds are crossed changes. In Case B, the interval $m_2^* \le m < m_1^*$ corresponds to an obligate-commensalism regime: The commensal cannot survive alone, but coexistence may still persist if $m < m_3^*$. In Case C, the coexistence equilibria disappear at $m = m_3^*$ before the host fold at $m = m_1^*$, leaving a host-only–extinction bistable phase. These possibilities are summarized in Table 4.

5. Basin of attraction analysis and global dynamical classification

5.1. Preliminary results

Lemma 5.1 (Boundedness)**.** *For any initial value* $(x_0, y_0) \in \mathbb{R}^2_{\geq 0}$*, the corresponding forward orbit of System* (1.1) *is bounded.*

Proof. For $y > \max\{A, L\}$, the product

$$\left(1 - \frac{y}{L}\right)\left(\frac{y}{A} - 1\right)$$

is negative, and hence, $G(y) < 0$. Therefore, $y(t)$ is ultimately bounded. If $y(t) \leq \bar{y}$, then

$$\dot{x} \leq -\frac{r}{K}x^2 + (r - mq_1E)x + b\bar{y}.$$

The right-hand side is negative for sufficiently large x, so $x(t)$ is also bounded.

Proposition 5.2 (Absence of nontrivial periodic orbits)**.** *System* (1.1) *admits no nonconstant periodic orbit in* $\mathbb{R}^2_{\geq 0}$*.*

Proof. If $(x(t), y(t))$ were periodic, then $y(t)$ would be a periodic solution of the scalar autonomous equation $\dot{y} = G(y)$. A one-dimensional autonomous equation has no nonconstant periodic solutions; hence, $y(t) \equiv \bar{y}$ for some equilibrium $\bar{y}$ of the host subsystem. Then, $x(t)$ satisfies the scalar autonomous equation $\dot{x} = F(x, \bar{y})$, which also has no nonconstant periodic solutions. Therefore, every periodic solution is an equilibrium.

Remark 5.3. This result provides a direct Bendixson-type complement to the asymptotically autonomous argument below. In particular, bounded trajectories cannot approach closed orbits; their long-term behavior is completely described by equilibria and their basins of attraction.

Proposition 5.4 (Global convergence of the host subsystem)**.** *For the scalar host equation* $\dot{y} = G(y)$*,*

(i) If $0 < m < m_1^*$*, then*

$$\lim_{t\to\infty} y(t) = 0 \quad \text{for } 0 \leq y(0) < y_1,$$

and

$$\lim_{t\to\infty} y(t) = y_2 \quad \text{for } y(0) > y_1.$$

Moreover, $y(t) \equiv y_1$ *if* $y(0) = y_1$*.*

(ii) If $m \geq m_1^*$*, then*

$$\lim_{t\to\infty} y(t) = 0$$

for all $y(0) \geq 0$ *except for the degenerate equilibrium* $y(0) = (L + A)/2$ *at* $m = m_1^*$*.*

Proof. Writing $G(y) = yH(y)$ gives

$$H(y) = -\frac{s}{AL}y^2 + \frac{s(L + A)}{AL}y - (s + mq_2E).$$

The sign pattern of this downward-opening quadratic is determined by the discriminant $\Delta_y(m)$. If $m < m_1^*$, H has two positive zeros $y_1 < y_2$, and the signs are negative, positive, negative on $(0, y_1)$, (y_1, y_2), and (y_2, ∞), respectively. If $m \geq m_1^*$, then $H(y) \leq 0$ for all $y \geq 0$. The conclusions follow from one-dimensional phase-line analysis.

Lemma 5.5 (Asymptotically autonomous limit)**.** *Consider a bounded solution of the triangular system*

$$\dot{x} = f(x, y), \qquad \dot{y} = g(y),$$

and suppose $y(t) \to y^*$ as $t \to \infty$. Then, its ω-limit set is contained in $\mathbb{R}_{\geq 0} \times \{y^*\}$ and is invariant under the limiting scalar equation

$$\dot{x} = f(x, y^*).$$

Proof. This is a standard consequence of the theory of asymptotically autonomous systems; see Thieme [34] and Mischaikow et al. [35]. Because $y(t) \to y^*$, the x-equation converges uniformly on compact time intervals to the limiting equation $\dot{x} = f(x, y^*)$, and the stated invariance of the ω-limit set follows.

5.2. Separatrix and basin classification

For $0 < m < m_1^*$, define

$$\mathcal{D}_5 = \{(x, y) \in \mathbb{R}^2_{\geq 0} : y > y_1\}, \qquad \mathcal{D}_{\text{ext}} = \{(x, y) \in \mathbb{R}^2_{\geq 0} : 0 \leq y < y_1\}.$$

Because the host equation is scalar and autonomous, the horizontal line $y = y_1$ is invariant and cannot be crossed by trajectories.

Proposition 5.6 (Separatrix)**.** *Assume $0 < m < \min\{m_1^*, m_3^*\}$. Then, the stable manifold of the saddle E_4 in the positive quadrant is*

$$\Gamma = W^s(E_4) \cap \mathbb{R}^2_{>0} = \{(x, y_1) : x > 0\}.$$

It separates the positive quadrant into the coexistence basin $\mathcal{D}_5$ and the extinction basin $\mathcal{D}_{\text{ext}}$.

Proof. The line $y = y_1$ is invariant because $G(y_1) = 0$. On this line, the x-equation reduces to the scalar equation $\dot{x} = F(x, y_1)$. Because $m < m_3^*$, $x = 0$ is repelling, and $x = x^*(y_1)$ is the unique positive attractor of this one-dimensional equation, every point (x, y_1) with $x > 0$ converges to E_4. Points with $y \neq y_1$ cannot converge to E_4 because the host component moves away from the invariant line according to the phase-line dynamics of Proposition 5.4.

On the invariant line $y = y_1$ itself, the one-dimensional x-dynamics has $x = 0$ (the point E_2) as a repeller when $m < m_3^*$, and $x = x^*(y_1)$ (the point E_4) is the unique attractor. Hence, the open segment $\{(x, y_1) : 0 < x < x^*(y_1)\}$ is precisely the portion of the one-dimensional unstable manifold of the source E_2 that lies along the invariant line $y = y_1$ and converges heteroclinically to the saddle E_4. This segment is part of the phase-portrait boundary structure and connects the two boundary equilibria on the y-axis.

Theorem 5.7 (Global dynamical classification)**.** *The global dynamics of System* (1.1) *is as follows.*

(I) If $0 < m < \min\{m_1^*, m_3^*\}$, the system is bistable. Initial values in $\mathcal{D}_5$ converge to

$$E_5 = (x^*(y_2), y_2),$$

whereas initial values in $\mathcal{D}_{\text{ext}}$ converge to E_1 if $m < m_2^*$ and to E_0 if $m \geq m_2^*$. The two basins are separated by $\Gamma = \{(x, y_1) : x > 0\}$.

(II) If $m_3^* \le m < m_1^*$, which can occur only in Case C, the coexistence equilibria no longer exist. The system exhibits host-only–extinction bistability: Trajectories with $y(0) > y_1$ tend to E_3, whereas those with $y(0) < y_1$ tend to E_0 or E_1 according to whether $m \ge m_2^*$ or $m < m_2^*$.

(III) If $m_1^* < m < m_2^*$, then the host collapses, and for $x(0) > 0$,

$$(x(t), y(t)) \to E_1 = (x_{\text{solo}}, 0).$$

At the fold value $m = m_1^*$, the same conclusion holds for all initial values except those lying on the degenerate invariant line $y = (L + A)/2$.

(IV) If $m \ge \max\{m_1^*, m_2^*\}$, and $m \ne m_1^*$, then

$$(x(t), y(t)) \to E_0 = (0, 0)$$

for all initial values in $\mathbb{R}^2_{\ge 0}$. At $m = m_1^*$, and the degenerate host equilibrium $y = (L + A)/2$ gives an exceptional invariant line.

Proof. The host limit is determined by Proposition 5.4. Once $y(t) \to y^*$, Lemma 5.5 reduces the limiting behavior of the commensal to the scalar equation $\dot{x} = F(x, y^*)$. For $y^* = y_2$, this scalar equation has the positive attractor $x^*(y_2)$ when $m < m_3^*$, and otherwise, $x = 0$ is attracting. For $y^* = 0$, it reduces to the harvested logistic equation

$$\dot{x} = x\left(r - mq_1E - \frac{r}{K}x\right),$$

whose positive equilibrium x_{solo} exists and attracts $(0, \infty)$ exactly when $m < m_2^*$. Combining these one-dimensional limits with the invariant separation by $y = y_1$ gives the stated classification.

Corollary 5.8. *Away from the fold value $m = m_1^*$, the system has a unique attracting equilibrium for all initial data with $x(0) > 0$ if and only if $m > m_1^*$. More precisely, the attractor is E_1 when $m_1^* < m < m_2^*$ and is E_0 when $m > \max\{m_1^*, m_2^*\}$. If $m < m_1^*$, the Allee threshold creates two distinct basins of attraction, and no single global attractor exists. At $m = m_1^*$, the degenerate invariant line $y = (L + A)/2$ corresponds to the fold point and must be treated separately.*

6. Bifurcation analysis

In this section, the harvesting parameter m is taken as the bifurcation parameter. The three thresholds m_1^*, m_2^*, and m_3^* correspond respectively to a fold bifurcation and two transcritical bifurcations.

Remark 6.1 (Applicability of Sotomayor's theorem)**.** Although the system is not C^1 at the origin $E_0 = (0, 0)$ due to the ratio-dependent benefit term (see Remark 2.1), this does not affect the rigorous applicability of Sotomayor's theorem to the three bifurcations analyzed below:

- The fold bifurcation at $m = m_1^*$ occurs at $\bar{y} = (L + A)/2 > 0$, far from the origin, where the vector field is smooth.

- Transcritical bifurcation I at $m = m_2^*$ takes place on the invariant axis $y = 0$, where the reduced one-dimensional equation $\dot{x} = x(r - mq_1E - rx/K)$ is smooth.
- Transcritical bifurcation II at $m = m_3^*$ involves collisions of E_2 with E_4 and E_3 with E_5 at points $(0, y_i)$ with $y_i > 0$ (because $m_3^* < m_1^*$ implies positive host roots), which lie strictly away from the origin in a region where the system is C^1.

Consequently, all three bifurcations satisfy the classical Sotomayor nondegeneracy conditions [39] in the usual analytical sense and are *analytical* transcritical/fold bifurcations, not merely topological ones.

6.1. Fold bifurcation at $m = m_1^*$

Theorem 6.2 (Fold bifurcation)**.** *At $m = m_1^*$, the positive host equilibria y_1 and y_2 coalesce at*

$$\bar{y} = \frac{L + A}{2}.$$

Consequently, E_2 and E_3 coalesce. If $m_1^* < m_3^*$, then the coexistence equilibria E_4 and E_5 also coalesce. This is a fold bifurcation.

Proof. For the host subsystem, positive equilibria are roots of

$$y^2 - (L + A)y + AL\left(1 + \frac{mq_2E}{s}\right) = 0.$$

At $m = m_1^*$, the discriminant vanishes, yielding the double root $\bar{y} = (L + A)/2$. Moreover,

$$G_m(\bar{y}, m_1^*) = -q_2E\bar{y} \neq 0, \qquad G_{yy}(\bar{y}, m_1^*) = -\frac{s(L + A)}{AL} \neq 0.$$

These are precisely the nondegeneracy conditions for a scalar fold bifurcation. The two-dimensional statement follows from the triangular structure.

6.2. Transcritical bifurcation I at $m = m_2^*$

Theorem 6.3 (Transcritical bifurcation I)**.** *At $m = m_2^*$, the commensal-only equilibrium E_1 collides with the origin E_0 on the invariant axis $y = 0$ and exchanges stability with it.*

Proof. On $y = 0$, the system reduces to

$$\dot{x} = x\left(r - mq_1E - \frac{r}{K}x\right).$$

Let $\mu = m - m_2^*$. Because $r - m_2^*q_1E = 0$, the reduced equation becomes

$$\dot{x} = -\mu q_1Ex - \frac{r}{K}x^2.$$

The nondegeneracy quantities are

$$f_{x\mu}(0, 0) = -q_1E \neq 0, \qquad f_{xx}(0, 0) = -\frac{2r}{K} \neq 0.$$

Thus, a transcritical bifurcation occurs at $m = m_2^*$.

6.3. Transcritical bifurcation II at $m = m_3^*$

Theorem 6.4 (Transcritical bifurcation II)**.** *At $m = m_3^*$, the coexistence equilibria collide with the boundary host equilibria:*

$$E_2 \leftrightarrow E_4, \qquad E_3 \leftrightarrow E_5,$$

whenever these equilibria exist. The stability in the commensal direction is exchanged.

Proof. At a positive host equilibrium $(0, y_i)$, the commensal-direction eigenvalue is

$$J_{11}(0, y_i) = r + \frac{b}{a} - mq_1E = q_1E(m_3^* - m).$$

Thus, it vanishes exactly at $m = m_3^*$. Taking the right and left eigenvectors as $\mathbf{w} = (1, 0)^T$ and $\mathbf{v} = (1, 0)^T$, we obtain

$$\mathbf{v}^T D\mathbf{f}_m \mathbf{w} = -q_1E \neq 0,$$

and

$$\mathbf{v}^T D^2\mathbf{f}(\mathbf{w}, \mathbf{w}) = -\frac{2r}{K} - \frac{2b}{a^2 y_i} \neq 0.$$

Hence, the Sotomayor nondegeneracy conditions for a transcritical bifurcation are satisfied.

6.4. Summary of the three bifurcations

Table 6 provides a quick comparison of the three bifurcations. Together with Table 4, it explains why different orderings of m_1^*, m_2^*, and m_3^* lead to different ecological scenarios.

Table 6. Summary of the three bifurcations induced by the harvesting parameter m.

Threshold & type	**Equilibria involved**	**Critical direction /eigenvectors**	**Nondegeneracy quantities**	**Ecological outcome**
$m = m_1^*$ (Fold)	$E_2 = E_3 = (0, \bar{y})$; if $m_1^* < m_3^*$, also $E_4 = E_5 = (\bar{x}, \bar{y})$.	For interior fold: $\mathbf{w} = (-\frac{J_{12}}{J_{11}}, 1)^T$, $\mathbf{v} = (0, 1)^T$.	$\mathbf{v}^T\mathbf{f}_m = -q_2E\bar{y} \neq 0$, $\mathbf{v}^T D^2\mathbf{f}(\mathbf{w}, \mathbf{w}) = -\frac{s(L+A)}{AL} \neq 0$.	Positive host equilibria collide and disappear; for $m > m_1^*$, host collapse occurs.
$m = m_2^*$ (Transcritical I)	E_1 and E_0 exchange stability on the invariant line $y = 0$.	Center direction along x; y-direction contracting. Near E_0: $\dot{x} = -\mu q_1 E x - \frac{r}{K}x^2$.	$f_{x\mu}(0, 0) = -q_1E \neq 0$, $f_{xx}(0, 0) = -\frac{2r}{K} \neq 0$.	Commensal-only equilibrium merges into the origin; the commensal loses the ability to survive independently.
$m = m_3^*$ (Transcritical II)	$E_2 \leftrightarrow E_4$ and $E_3 \leftrightarrow E_5$, when $m_3^* < m_1^*$.	At $(0, y_i)$: $\mathbf{w} = (1, 0)^T$, $\mathbf{v} = (1, 0)^T$.	$\mathbf{v}^T D\mathbf{f}_m \mathbf{w} = -q_1E \neq 0$, $\mathbf{v}^T D^2\mathbf{f}(\mathbf{w}, \mathbf{w}) = -\frac{2r}{K} - \frac{2b}{a^2 y_i} \neq 0$.	Coexistence equilibria disappear; boundary host equilibria reverse their stability in the commensal direction.

7. Numerical examples

We now illustrate the theoretical results with the parameter set

$$\begin{gathered} r = 0.5, \quad K = 100, \quad b = 0.3, \quad a = 50, \quad q_1 = q_2 = 0.3, \\ s = 0.4, \quad L = 100, \quad A = 40, \quad E = 1. \end{gathered} \tag{7.1}$$

7.1. Critical thresholds

Substitution of (7.1) into the threshold formulas gives

$$m_1^* = 0.3000, \qquad m_2^* \approx 1.6667, \qquad m_3^* \approx 1.6867. \tag{7.2}$$

Thus, the baseline ordering is

$$m_1^* < m_2^* < m_3^*,$$

which corresponds to Case A in Table 4. Therefore, as m increases, the system passes through three observable regimes:

bistability $\longrightarrow$ host collapse with commensal-only survival $\longrightarrow$ complete extinction.

7.2. Sensitivity of the critical thresholds to A and q_1/q_2

The three thresholds are explicitly given by

$$m_1^* = \frac{s(L-A)^2}{4ALq_2E}, \qquad m_2^* = \frac{r}{q_1E}, \qquad m_3^* = \frac{r + b/a}{q_1E}.$$

Hence, the Allee threshold A mainly affects the host fold threshold m_1^*, whereas the catchability coefficient q_1 rescales the two commensal-related thresholds m_2^* and m_3^*.

Table 7. Sensitivity of m_1^* to the Allee threshold A.

A	m_1^*	m_2^*	m_3^*	Ordering
20	1.0667	1.6667	1.6867	Case A
40	0.3000	1.6667	1.6867	Case A
60	0.0889	1.6667	1.6867	Case A
80	0.0167	1.6667	1.6867	Case A

Table 7 shows that increasing the Allee threshold A decreases m_1^* substantially, making the host more vulnerable to harvesting-induced collapse.

Table 8. Sensitivity of the threshold ordering to the catchability ratio q_1/q_2.

q_1	q_1/q_2	m_1^*	m_2^*	m_3^*	Ordering
0.30	1.000	0.3000	1.6667	1.6867	Case A
1.00	3.333	0.3000	0.5000	0.5060	Case A
1.68	5.600	0.3000	0.2976	0.3012	Case B
1.70	5.667	0.3000	0.2941	0.2976	Case C

For the baseline values, the transitions between Cases A, B, and C occur near the critical ratios

$$\frac{q_1}{q_2} \approx 5.556 \quad \text{and} \quad \frac{q_1}{q_2} \approx 5.622.$$

Thus moderate changes in q_1/q_2 preserve the baseline ordering, whereas a sufficiently large commensal catchability can move the system into Case B or Case C.

7.3. *Low harvesting regime:* $m = 0.15$

For $m = 0.15 < m_1^*$, the host subsystem has two positive equilibria

$$y_1 \approx 48.79, \qquad y_2 \approx 91.21.$$

The commensal-only equilibrium and coexistence equilibria are

$$E_1 = (91.0, 0), \qquad E_4 \approx (92.16, 48.79), \qquad E_5 \approx (92.18, 91.21).$$

Consistent with Table 5, E_1 and E_5 are stable nodes, whereas E_4 is a saddle. The separatrix is the horizontal line

$$\Gamma = \{(x, y) : y = y_1,\ x > 0\},$$

which divides the extinction basin from the coexistence basin. The corresponding phase portrait is shown in Figure 1.

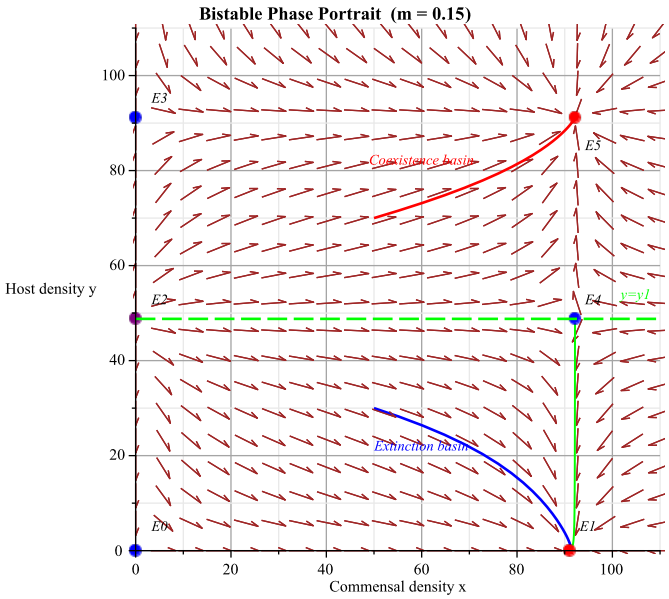

Figure 1. Bistable phase portrait ($m = 0.15$). Red filled circles denote the stable equilibria E_1, E_5; blue filled circles denote the saddles E_0, E_3, E_4; the purple filled circle denotes the source E_2. The green dashed line $y = y_1 \approx 48.79$ is the separatrix Γ. Trajectory 1 (initial values $x(0) = 50,\ y(0) = 30$) converges to E_1; Trajectory 2 (initial values $x(0) = 50,\ y(0) = 70$) converges to E_5.

7.4. *Fold Bifurcation:* $m = m_1^* = 0.3$

At $m = m_1^* = 0.3$, the two positive host equilibria merge at

$$\bar{y} = \frac{L + A}{2} = 70.$$

Thus, E_2 and E_3 coalesce, and because $m_1^* < m_3^*$, the coexistence equilibria E_4 and E_5 coalesce, as well. The host-coordinate bifurcation diagram is shown in Figure 2, and the corresponding commensal-coordinate bifurcation diagram is shown in Figure 3.

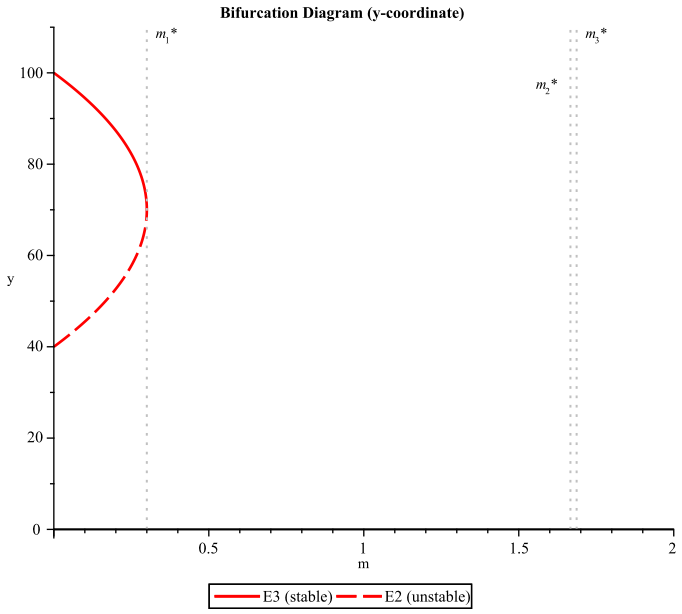

Figure 2. Bifurcation diagram of host y-coordinates vs. m. A fold bifurcation occurs at $m = m_1^*$, where y_1, y_2 (and hence E_2, E_3 and E_4, E_5) merge and annihilate.

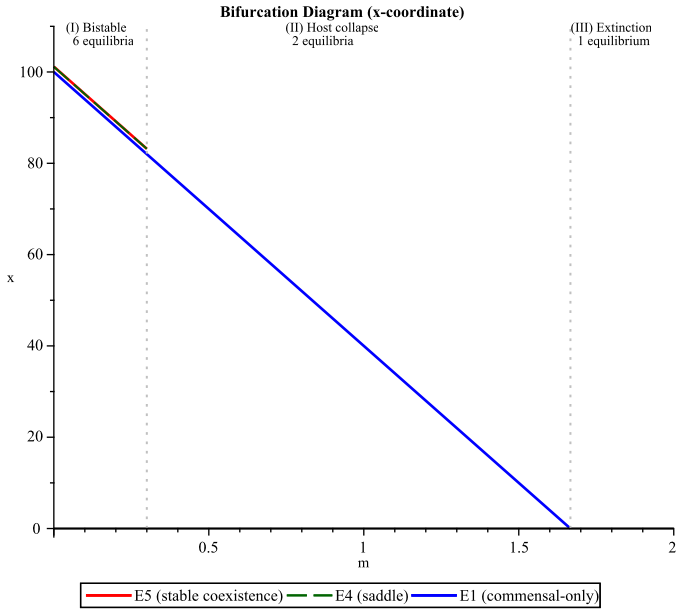

Figure 3. Bifurcation diagram of commensal x-coordinates vs. m. A transcritical bifurcation occurs at $m = m_2^*$, where E_1 merges into E_0 (both lie on $y = 0$). Shaded regions mark the dynamical regimes (i)–(iii).

7.5. *Medium harvesting regime:* $m = 0.5$

For $m = 0.5 \in [m_1^*, m_2^*)$, the host has no positive equilibrium, and every positive host trajectory satisfies $y(t) \to 0$. Meanwhile,

$$x_{\text{solo}} = 100\left(1 - \frac{0.5 \times 0.3}{0.5}\right) = 70.$$

Hence, trajectories with $x(0) > 0$ converge to

$$E_1 = (70, 0).$$

This host-collapse regime is illustrated in Figure 4.

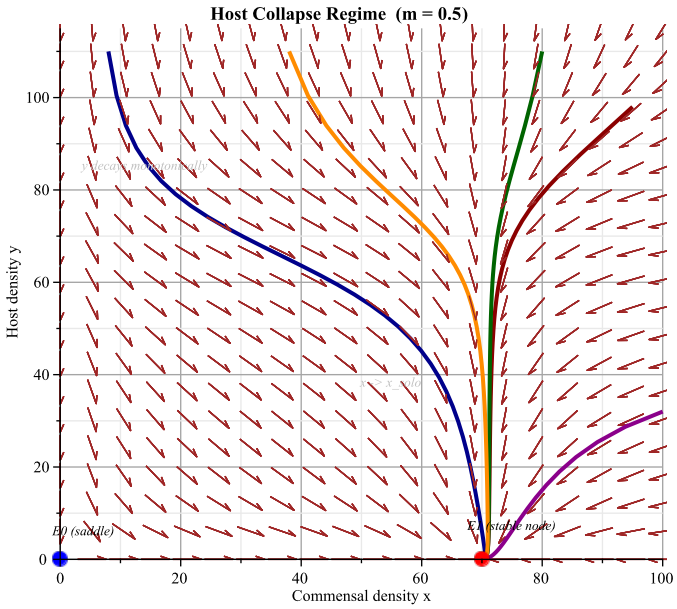

Figure 4. Phase portrait in the host collapse regime ($m = 0.5$). The host has no nonzero equilibria, and $y(t)$ decays monotonically to zero. E_0 is a saddle, and $E_1 = (70, 0)$ is a globally attracting stable node. Five trajectories with diverse initial conditions ($(8, 110)$, $(38, 110)$, $(80, 110)$, $(95, 98)$, $(100, 32)$) are shown; all converge to E_1.

7.6. *High harvesting regime:* $m = 1.68$

For $m = 1.68 > m_2^*$, the commensal-only equilibrium no longer exists, and $m > m_1^*$ implies host collapse. Thus, the origin is the unique equilibrium and is globally attracting:

$$(x(t), y(t)) \to E_0 = (0, 0).$$

Harvesting pressure ultimately drives both populations to complete extinction. The corresponding phase portrait is shown in Figure 5.

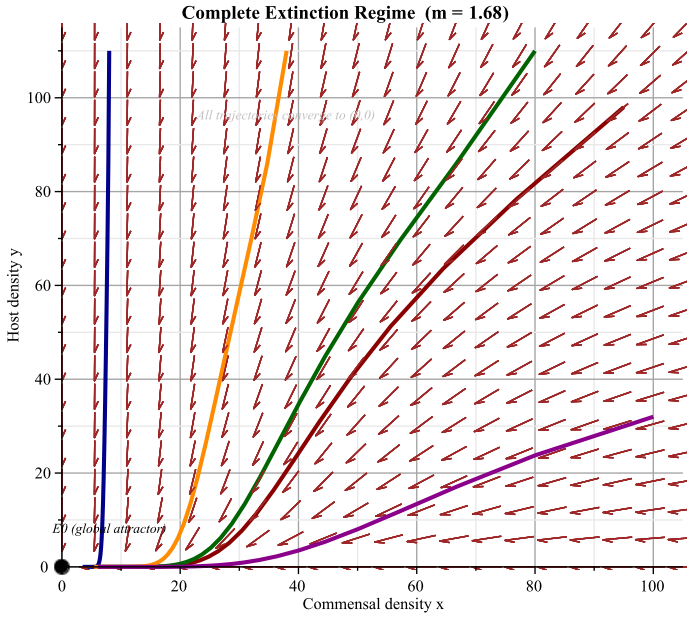

Figure 5. Phase portrait in the complete extinction regime ($m = 1.68$). The sole remaining equilibrium is $E_0 = (0, 0)$, which is a globally attracting stable node. Five trajectories starting from $(8, 110)$, $(38, 110)$, $(80, 110)$, $(95, 98)$, and $(100, 32)$ all converge to the origin.

7.7. Transcritical bifurcation I

At $m = m_2^* \approx 1.667$, the commensal-only equilibrium satisfies $x_{\text{solo}} \to 0$ and collides with E_0 on the invariant line $y = 0$. This is precisely the transcritical bifurcation proved in Theorem 6.3. The transition is visible in the commensal-coordinate bifurcation diagram in Figure 3.

7.8. Summary of graphical results (Figures 1–5)

Figures 1–5 correspond to the five dynamical regimes listed in Table 9 and collectively illustrate the full spectrum of behaviors predicted by the theoretical analysis.

- **Figure 1 (Low harvesting, $m = 0.15$).** This phase portrait exhibits the bistable regime with all six equilibria present. The horizontal separatrix $\Gamma = \{(x, y) : y = y_1, \ x > 0\}$ (green dashed line) divides the phase plane: Trajectories initialized below y_1 converge to the commensal-only attractor E_1, whereas those above y_1 converge to the stable coexistence equilibrium E_5. The saddle E_4 lies at the intersection of the separatrix with the commensal nullcline, and the source E_2 at $(0, y_1)$ repels trajectories along the separatrix toward E_4. This confirms the basin separation predicted by Proposition 5.6 and Theorem 5.7(I).

- **Figure 2 (Fold bifurcation diagram).** This bifurcation diagram tracks the host equilibrium coordinates y_1 and y_2 as functions of the harvesting parameter m. As m increases, the two branches approach each other and merge at the fold point $m = m_1^* = 0.3$, where $y_1 = y_2 = \bar{y} = 70$. For $m > m_1^*$, no positive host equilibrium exists, confirming the fold bifurcation analyzed in

Theorem 6.2. The upper branch (y_2) represents the stable host carrying capacity, and the lower branch (y_1) is the unstable Allee threshold.

- **Figure 3 (Transcritical bifurcation diagram).** This diagram displays the commensal equilibrium coordinates x_{solo}, $x^*(y_1)$, and $x^*(y_2)$ versus m. The commensal-only equilibrium x_{solo} decreases linearly with m and vanishes at the transcritical bifurcation point $m = m_2^* \approx 1.667$, where it collides with the origin E_0. Meanwhile, the coexistence equilibria E_4 and E_5 merge at the fold point $m = m_1^*$ and disappear. This diagram visually confirms both Theorem 6.3 (transcritical I) and the fold-induced disappearance of coexistence states.
- **Figure 4 (Host collapse, $m = 0.5$).** For harvesting above the fold threshold ($m_1^* < m < m_2^*$), the host has no positive equilibrium, and all host trajectories satisfy $y(t) \to 0$. The phase portrait shows that regardless of initial host density, the commensal converges to the commensal-only equilibrium $E_1 = (70, 0)$, and the host undergoes monotonic extinction. This illustrates the monostable host-collapse regime described in Theorem 5.7(III).
- **Figure 5 (Complete extinction, $m = 1.68$).** Under strong harvesting ($m > m_2^*$), both the host positive equilibria and the commensal-only equilibrium are absent, leaving $E_0 = (0, 0)$ as the unique global attractor. All trajectories converge to the origin, confirming the complete extinction predicted by Theorem 5.7(IV). This regime illustrates the ecological risk of excessive harvesting pressure in systems with Allee effects.

In summary, Figures 1–5 provide a complete visual verification of the theoretical results: the bistable structure at low harvesting, the fold bifurcation that destroys positive host states, the transcritical bifurcation that eliminates commensal survival, and the eventual collapse to monostability and extinction as harvesting intensifies.

Table 9. Numerical regimes for the baseline parameter set.

m value	Regime	No. of equilibria	Attractor(s)	Figure
0.15	Low harvesting	6	E_1 or E_5	Figure 1
0.30	Fold point	4	Nonhyperbolic	Figures 2 and 3
0.50	Host collapse	2	E_1	Figure 4
1.667	Transcritical I	1	Nonhyperbolic	Figure 3
1.68	Complete extinction	1	E_0	Figure 5

The numerical results agree with the theoretical equilibrium classification, global basin structure, and bifurcation analysis. The corresponding numerical data are compiled in Table 9.

8. Discussion and outlook

This paper has analyzed a host–commensal system with a multiplicative Allee effect on the host and nonselective harvesting on both species. The central mathematical feature is the triangular structure of the system: The host equation is independent of the commensal variable. This structure makes it possible to reduce the equilibrium classification, local stability analysis, global basin description, and bifurcation verification to one-dimensional problems.

The analysis identifies three critical harvesting thresholds:

$$m_1^* = \frac{s(L-A)^2}{4ALq_2E}, \qquad m_2^* = \frac{r}{q_1E}, \qquad m_3^* = \frac{r+b/a}{q_1E}.$$

The threshold m_1^* corresponds to the disappearance of positive host equilibria through a fold bifurcation; m_2^* corresponds to the loss of commensal-only survival through a transcritical bifurcation; and m_3^* corresponds to the loss of commensal invasion ability around positive host states. Depending on the ordering of these thresholds, the system may exhibit coexistence–commensal-only bistability, coexistence–extinction bistability, or host-only–extinction bistability. In the baseline ordering $m_1^* < m_2^* < m_3^*$, harvesting first destroys the positive host equilibria and then eliminates the commensal-only state, leading eventually to complete extinction.

Compared with commensalism models with purely logistic host growth, the multiplicative Allee effect creates a sharp threshold structure in the host dimension. The separatrix $y = y_1$ divides the basin of coexistence from the basin of collapse. From a management perspective, this means that harvesting pressure should be kept below m_1^* if stable coexistence is desired; once m crosses this value, the positive host equilibria disappear, and the system undergoes a critical transition from bistability to monostability.

Several limitations and extensions deserve further investigation. First, the present model assumes strictly asymmetric commensalism: The host is not affected by the commensal. This assumption yields the triangular structure used in the complete analysis. In natural systems, however, weak feedback from the commensal to the host may occur. Introducing such feedback would destroy the exact cascade reduction, although hyperbolic equilibria are expected to persist under sufficiently small perturbations.

Second, the bistable regime raises several management-oriented questions. One may formulate an optimal harvesting problem that maximizes long-term yield while keeping the host density above the separatrix $y = y_1$. Resilience indices, such as distance to the separatrix and recovery time after perturbations, would also provide useful early-warning indicators for Allee-induced collapse. A comparison between multiplicative and additive Allee formulations is another natural extension.

Third, temporal delays are common in ecological systems because reproduction, maturation, harvesting response, and commensal benefit may not be instantaneous. Delayed harvesting predator–prey models with multiple delays can generate positive periodic solutions and more complicated long-term behaviors [40]. Incorporating delay into the present framework may therefore lead to Hopf bifurcations and delay-induced oscillations.

Finally, harvesting decisions are often coupled with economic factors. Eco-economic or bioeconomic systems, including differential-algebraic models with economic constraints, can exhibit rich bifurcation phenomena [41]. Combining the present Allee-threshold-driven commensal system with profit, cost, and effort dynamics would provide a more realistic framework for sustainable harvesting policy. Stochastic perturbations and spatial dispersal also remain important directions for future work.

Use of AI tools declaration

The authors used an AI-based language tool only for language polishing and formatting suggestions. The authors take full responsibility for the content, mathematical results, and conclusions of the manuscript.

Acknowledgments

This research was funded by Industry-University-Research Project of West Anhui University (2026: Development of Agricultural Product Yield Prediction Model Based on Nonlinear Dynamics Algorithm), the Humanities and Social Sciences Key Grant Foundation of the Education Department of Anhui Province of China (No.2024AH053477) and the Humanities and Social Sciences Key Project of the Anhui Provincial Department of Education (No.2025AHGXSK30179).

Conflict of interest

The authors declare that there are no conflicts of interest.

References

1. P. Quansah, M. Ibrahim, Global dynamics of a ratio-dependent commensalism model with nonselective harvesting and partial closure for the populations, *J. Math. Comput. Sci.*, **16** (2026), 2. https://doi.org/10.28919/jmcs/9762
2. R. Fawthrop, J. Cerca, G. Pacheco, G. Satre, E. S. C. Scordato, M. Ravinet, et al., Understanding human-commensalism through an ecological and evolutionary framework, *Trends Ecol. Evol.*, **40** (2025), 159–169. https://doi.org/10.1016/j.tree.2024.10.006
3. A. Mougi, The roles of amensalistic and commensalistic interactions in large ecological network stability, *Sci. Rep.*, **6** (2016), 29929. https://doi.org/10.1038/srep29929
4. T. Li, Q. Wang, Bifurcation analysis for two-species commensalism (amensalism) systems with distributed delays, *Int. J. Bifurcation Chaos*, **32** (2022), 2250133. https://doi.org/10.1142/S0218127422501334
5. Y. Chong, A. J. Kashyap, S. Chen, F. Chen, Dynamics analysis of a discrete-time commensalism model with additive Allee effect for the host species, *Axioms*, **12** (2023), 1031. https://doi.org/10.3390/axioms12111031
6. E. C. D. Stewart, N. Jimi, C. Moreau, T. G. Dahlgren, A. G. Glover, Novel deep-sea commensalism: a new genus and two new species of Myzostomida from the abyssal Pacific Ocean, *Invertebr. Syst.*, **40** (2026), IS25078. https://doi.org/10.1071/IS25078
7. K. A. Mathis, J. L. Bronstein, Our current understanding of commensalism, *Annu. Rev. Ecol. Evol. Syst.*, **51** (2020), 167–189. https://doi.org/10.1146/annurev-ecolsys-011720-040844
8. C. R. Dickman, Body size, prey size, and community structure in insectivorous mammals, *Ecology*, **69** (1988), 569–580. https://doi.org/10.2307/1941006
9. X. He, Z. Zhu, J. Chen, F. Chen, Dynamical analysis of a Lotka–Volterra commensalism model with additive Allee effect, *Open Math.*, **20** (2022), 646–665. https://doi.org/10.1515/math-2022-0055
10. L. Xu, Y. Xue, Q. Lin, C. Lei, Global attractivity of symbiotic model of commensalism in four populations with Michaelis–Menten type harvesting in the first commensal populations, *Axioms*, **11** (2022), 337. https://doi.org/10.3390/axioms11070337

11. P. Lemes, F. G. Barbosa, B. Naimi, M. B. Araújo, Dispersal abilities favor commensalism in animal–plant interactions under climate change, *Sci. Total Environ.*, **835** (2022), 155157. https://doi.org/10.1016/j.scitotenv.2022.155157
12. R. Wu, L. Li, Dynamic behaviors of a commensal symbiosis model with ratio-dependent functional response and one party cannot survive independently, *J. Math. Comput. Sci.*, **16** (2016), 495–506. https://doi.org/10.22436/jmcs.016.04.03
13. W. C. Allee, Animal aggregations, *Q. Rev. Biol.*, **2** (1927), 367–398. https://doi.org/10.1086/394281
14. F. Courchamp, T. Clutton-Brock, B. Grenfell, Inverse density dependence and the Allee effect, *Trends Ecol. Evol.*, **14** (1999), 405–410. https://doi.org/10.1016/S0169-5347(99)01683-3
15. P. A. Stephens, W. J. Sutherland, Consequences of the Allee effect for behaviour, ecology and conservation, *Trends Ecol. Evol.*, **14** (1999), 401–405. https://doi.org/10.1016/S0169-5347(99)01684-5
16. K. Fang, Y. Wang, F. Chen, X. Chen, Dynamics of a modified Lotka–Volterra commensalism system incorporating Allee effect and symmetric nonselective harvest, *Symmetry*, **17** (2025), 852. https://doi.org/10.3390/sym17060852
17. J. Zhong, L. Chen, F. Chen, Stability and bifurcation in a two-patch commensal symbiosis model with nonlinear dispersal and additive Allee effect, *Int. J. Biomath.*, **19** (2026), 2450099. https://doi.org/10.1142/S1793524524500992
18. M. B. Almatrafi, Stability and period-doubling bifurcation of fractional-order commensal symbiosis model with Allee effect, *Fractal Fract.*, **10** (2026), 226. https://doi.org/10.3390/fractalfract10040226
19. S. Işık, Stability and period-doubling bifurcation in a modified commensal symbiosis model with Allee effect, *Erzincan Univ. J. Sci. Technol.*, **15** (2022), 310–324. https://doi.org/10.18185/erzifbed.879963
20. A. Tassaddiq, R. Ahmed, A. Ditta, Exploring stability and bifurcation in a discretized commensalism model, *Nonlinear Dyn.*, **113** (2025), 28463–28475. https://doi.org/10.1007/s11071-025-11530-4
21. P. Georgescu, D. Maxin, H. Zhang, Global stability results for models of commensalism, *Int. J. Biomath.*, **10** (2017), 1750037. https://doi.org/10.1142/S1793524517500371
22. F. Courchamp, L. Berec, J. Gascoigne, *Allee Effects in Ecology and Conservation*, Oxford University Press, 2008. https://doi.org/10.1093/acprof:oso/9780198570301.001.0001
23. L. Berec, E. Angulo, F. Courchamp, Multiple Allee effects and population management, *Trends Ecol. Evol.*, **22** (2007), 185–191. https://doi.org/10.1016/j.tree.2006.12.002
24. L. Zhao, J. Shen, Canards and homoclinic orbits in a slow-fast modified May–Holling–Tanner predator-prey model with weak multiple Allee effect, *Discrete Contin. Dyn. Syst. - Ser. B*, **27** (2022), 6745–6769. https://doi.org/10.3934/dcdsb.2022018
25. F. Kangalgil, M. Altunkaynak, Chaos control and bifurcations in a modified discrete prey–predator model with weak multiple Allee effect, *Int. J. Bifurcation Chaos*, **35** (2025), 2550124. https://doi.org/10.1142/S021812742550124X

26. J. Xiao, Y. Xia, Spatiotemporal dynamics in a diffusive predator-prey model with multiple Allee effect and herd behavior, *J. Math. Anal. Appl.*, **529** (2024), 127569. https://doi.org/10.1016/j.jmaa.2023.127569
27. C. W. Clark, *Mathematical Bioeconomics: The Optimal Management of Renewable Resources*, Wiley, 1990.
28. A. Ditta, P. A. Naik, R. Ahmed, Z. Huang, Exploring periodic behavior and dynamical analysis in a harvested discrete-time commensalism system, *Int. J. Dyn. Control*, **13** (2025), 63. https://doi.org/10.1007/s40435-024-01551-z
29. S. Jawad, Study the dynamics of commensalism interaction with Michaelis–Menten type prey harvesting, *Al-Nahrain J. Sci.*, **25** (2022), 45–50. https://doi.org/10.22401/ANJS.25.1.08
30. C. Lu, X. Liu, Z. Li, The dynamics and harvesting strategies of a predator-prey system with Allee effect on prey, *AIMS Math.*, **8** (2023), 28897–28925. https://doi.org/10.3934/math.20231481
31. H. Liu, H. Yu, C. Dai, Z. Ma, Q. Wang, M. Zhao, Dynamical analysis of an aquatic amensalism model with nonselective harvesting and Allee effect, *Math. Biosci. Eng.*, **18** (2021), 8857–8882. https://doi.org/10.3934/mbe.2021437
32. N. Min, P. Xing, H. Zhang, Role of Allee effect, hunting cooperation, and prey harvesting in a Leslie–Gower predator–prey model, *Adv. Contin. Discrete Models*, **2025** (2025), 96. https://doi.org/10.1186/s13662-025-03951-7
33. P. Sardar, S. Biswas, K. P. Das, S. Rana, B. Pal, F. Ali, et al., Exploring multiple bifurcation behaviors and chaos control via weak Allee effect and harvesting in a predator–prey interaction model, *Nonlinear Sci.*, **4** (2025), 100033. https://doi.org/10.1016/j.nls.2025.100033
34. H. R. Thieme, Convergence results and a Poincaré–Bendixson trichotomy for asymptotically autonomous differential equations, *J. Math. Biol.*, **30** (1992), 755–763. https://doi.org/10.1007/BF00173267
35. K. Mischaikow, H. L. Smith, H. R. Thieme, Asymptotically autonomous semiflows: chain recurrence and Lyapunov functions, *Trans. Am. Math. Soc.*, **347** (1995), 1669–1685. https://doi.org/10.1090/S0002-9947-1995-1290727-7
36. F. Chen, Y. Chen, Z. Li, L. Chen, Note on the persistence and stability property of a commensalism model with Michaelis–Menten harvesting and Holling type II commensalistic benefit, *Appl. Math. Lett.*, **134** (2022), 108381. https://doi.org/10.1016/j.aml.2022.108381
37. M. W. Hirsch, Systems of differential equations which are competitive or cooperative. I: Limit sets, *SIAM J. Math. Anal.*, **13** (1982), 167–179. https://doi.org/10.1137/0513013
38. H. L. Smith, *Monotone Dynamical Systems: An Introduction to the Theory of Competitive and Cooperative Systems*, American Mathematical Society, 1995.
39. J. Sotomayor, Generic bifurcations of dynamical systems, in *Dynamical Systems*, (1973), 561–582. https://doi.org/10.1016/B978-0-12-550350-1.50047-3
40. G. Zhang, Y. Shen, B. Chen, Positive periodic solutions in a nonselective harvesting predator–prey model with multiple delays, *J. Math. Anal. Appl.*, **395** (2012), 298–306. https://doi.org/10.1016/j.jmaa.2012.05.045

41. G. Zhang, H. Guo, L. Wang, Exploring bifurcations in a differential-algebraic model of predator–prey interactions, *Nonlinear Dyn.*, **112** (2024), 20549–20571. https://doi.org/10.1007/s11071-024-10098-9

AIMS Press